

# Mechanically Stable Intraspinal Microstimulation Implants for Human Translation

AMIRALI TOOSI,<sup>1,4</sup> DIRK G. EVERAERT,<sup>2,4</sup> AUSTIN AZAR,<sup>3,4</sup> CHRISTOPHER R. DENNISON,<sup>3,4</sup>  
and VIVIAN K. MUSHAHWAR<sup>1,2,4</sup>

<sup>1</sup>Neuroscience and Mental Health Institute, University of Alberta, 5005 Katz Building, Edmonton, AB T6G 2E1, Canada;  
<sup>2</sup>Division of Physical Medicine and Rehabilitation, Department of Medicine, University of Alberta, Edmonton, AB, Canada;  
<sup>3</sup>Biomedical Instrumentation Lab, Department of Mechanical Engineering, University of Alberta, Edmonton, AB, Canada; and  
<sup>4</sup>Alberta Innovates – Health Solutions Interdisciplinary Team in Smart Neural Prostheses (Project SMART), Edmonton, AB, Canada

(Received 16 April 2016; accepted 8 August 2016; published online 25 August 2016)

Associate Editor Xiaoxiang Zheng oversaw the review of this article.

**Abstract**—The goal of this study was to develop stable intraspinal microstimulation (ISMS) implants for use in humans to restore standing and walking after spinal cord injury. ISMS electrically activates locomotor networks within the lumbar region of the spinal cord. In animals, ISMS produced better functional outcomes than those obtained by other interventions, and recent efforts have focused on translating this approach to humans. This study used domestic pigs to: (1) quantify the movements and length changes of the implant region of the spinal cord during spine flexion and extension movements; and (2) measure the forces leading to the dislodgement of the ISMS electrodes. The displacement of the spinal cord implant region was  $5.66 \pm 0.57$  mm relative to the implant fixation point on the spine. The overall length change of the spinal cord implant region was  $5.64 \pm 0.59$  mm. The electrode dislodgement forces were  $60.9 \pm 35.5$  mN. Based on these results, six different coil types were fabricated and their strain relief capacity assessed. When interposed between the electrodes and the stimulator, five coil types successfully prevented the dislodgement of the electrodes. The results of this study will guide the design of mechanically stable ISMS implants for ultimate human use.

**Keywords**—Intraspinal implant, Dislodgment forces, Lumbar spine biomechanics, Strain relief, Coiled lead wire.

## ABBREVIATIONS

FES      Functional electrical stimulation

FBR      Foreign body response  
ISMS      Intraspinal microstimulation  
SCI      Spinal cord injury

## INTRODUCTION

Spinal cord injury (SCI) affects 250,000–500,000 people around the world each year.<sup>37</sup> Depending on the type and level of injury, SCI can result in loss of control over various parts of the body such as the limbs and bladder.<sup>37</sup> One of the successful approaches for restoring lost functions after SCI is functional electrical stimulation (FES).<sup>26</sup> Intraspinal microstimulation (ISMS) is an FES technique that delivers electrical pulses directly to the ventral horn of the spinal cord. It has the potential to restore standing and walking after SCI by targeting the lumbar enlargement of the spinal cord, which contains neural networks responsible for controlling the movements of the legs.

Movements elicited by ISMS implants in the lumbar enlargement have been extensively studied in animal models (e.g., cats<sup>16,20,21,29</sup> and rats<sup>2,3</sup>) and show positive outcomes such as the production of functional weight-bearing fatigue-resistant movements in the legs after complete SCI,<sup>29</sup> and production of long durations of standing<sup>16</sup> and long distances of propulsive over-ground walking in anesthetized animals.<sup>12</sup> These results suggest that ISMS is a promising approach for restoring functional leg movements after SCI in humans.

Implants for ISMS in the lumbar cord comprise an array of penetrating electrodes with tips reaching the

Address correspondence to Vivian K. Mushahwar, Neuroscience and Mental Health Institute, University of Alberta, 5005 Katz Building, Edmonton, AB T6G 2E1, Canada. Electronic mail: vivian.mushahwar@ualberta.ca

ventral horn, an electrical stimulator that generates the electrical pulses, and lead wires that connect the electrodes to the stimulator (Fig. 1). The mechanical stability of the implant in chronic studies conducted in cats<sup>20</sup> and rats<sup>3</sup> has been a critical factor in the long-term functional success of this approach.<sup>1</sup> In those studies, small amounts of slack in the lead wires accommodated for the small movements of the implant region of the spinal cord relative to the spine. Mushahwar *et al.*<sup>20</sup> demonstrated that at least two thirds of chronically implanted ISMS electrodes remain functional in intact, awake cats for periods up to 6 months (longest tested). Similarly, Bamford *et al.*<sup>3</sup> demonstrated that more than 90% of chronically implanted ISMS electrodes stay functional up to 30 days in rats (longest tested).

Sacral ISMS implants have been implemented in humans after SCI. In 1972, Nashold *et al.*<sup>22,23</sup> reported the first clinical implementation of an ISMS implant in 11 patients for restoring bladder function. Two electrodes were implanted subdurally, one in each side of the spinal cord. The electrodes were embedded in a silastic base, and connected to flexible multi-strand stainless steel lead-wires. The lead wires laid on the dorsal surface of the cord and in turn connected to an implanted stimulator. To stabilize the electrodes, a silastic-coated strap fixed to the electrode base was wrapped around the spinal cord. In the five-year follow up,<sup>23</sup> implants in 10 patients had remained functional without displacement or dislodgment from their initial

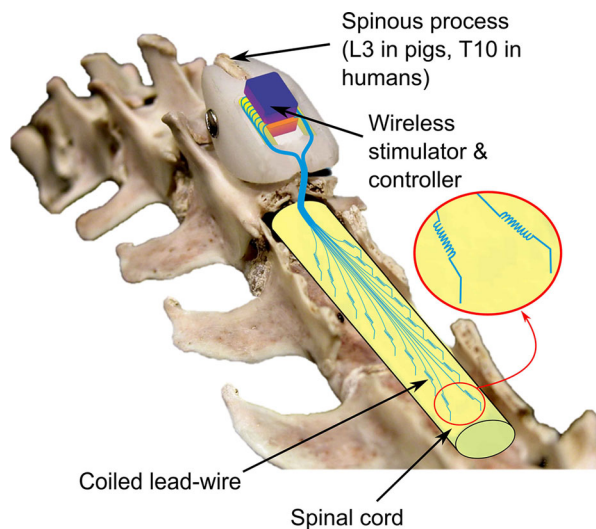


**FIGURE 1.** Conceptual representation of an ISMS implant. The implant consists of electrodes implanted in the spinal cord with tips reaching the ventral horn, a stimulator, and lead wires connecting the electrodes to the stimulator. This study focused on incorporating a strain relief mechanism (coils) in the lead wires to minimize the effect of relative movement between the spinal column and spinal cord on the implanted electrodes.

position. In one patient, the connection between the implanted electrodes and the stimulator had broken, and one of the electrodes had dislodged from the spinal cord.

Translating ISMS to a lumbar implant for restoring standing and walking is more challenging. This is partly due to the number of electrodes in a lumbar ISMS implant (16–24 vs. only 2) and the size of the implant region (5 cm for lumbar vs. ~1 cm for sacral). To ensure that the implanted electrodes remain stable in the spinal cord, an appropriately designed strain relief mechanism in the lead wires connecting the electrodes to the stimulator is necessary to prevent the transmission of forces to the electrodes during natural movements of the spine.

In addition to maintaining electrode stability, the strain relief mechanism should mechanically disengage the electrodes that are floating within the soft tissue of the spinal cord from the surrounding hard bones. The mechanical interaction of electrodes with surrounding tissue is an important consideration in neural implants.<sup>1</sup> Biran *et al.*<sup>4</sup> demonstrated that microelectrodes implanted in the brain and tethered to the skull result in significantly larger reactivity in the nervous tissue than untethered microelectrodes. This increased reactivity may be due to the relative motion of the tethered electrode with respect to its surrounding tissue, and could be the cause of local neurodegeneration.<sup>4,18</sup> Motion of the implanted electrodes relative to surrounding tissue may be caused by rhythmic physiological movements of the tissue such as breathing and blood flow pulsations, or from movements of body parts activated by the implant itself. Lead-wire designs that resemble untethered conditions as closely as possible are needed to minimize these deleterious relative motions.

This study focused on the design of lead wires for ISMS implants with a coil for strain relief that not only guarantees stability of the implants, but also in effect mechanically dissociates the floating implanted electrodes from the fixed implanted stimulator (Fig. 1). The coil required a high degree of flexibility and extensibility to minimize the relative motion between the electrode and surrounding tissue, and maintain the electrode stably in place. The design constraints were systematically identified in an animal model with spine mechanics that closely resembled those of humans. These constraints were: (1) the elongation and displacement of the spinal cord relative to the surrounding spinal vertebrae during physiological motions in order to determine the required range of coil movement; and (2) the forces that lead to electrode dislodgement which should not be reached within the range of coil movement. Domestic pigs, commonly used in spine research,<sup>5,31</sup> were chosen as the animal

model because of the similarity of their spinal column anatomy<sup>5,30</sup> and range of motion<sup>38</sup> to that of humans. To the best of our knowledge, this study not only provides the first design specifications for a strain relief mechanism for a neural implant in the spinal cord, but also provides detailed analysis of the biomechanics of the spine and spinal column of pigs during physiological movements.

## MATERIALS AND METHODS

Studies were conducted in a total of six fresh domestic pig cadavers (48–54 kg). Three cadavers were used to establish the techniques and collect pilot data for the design of different coil types. After finalizing the methods, the remaining three pig cadavers were used to collect the results presented in this manuscript. In all of these experiments, the *in situ* dislodgment trials ([Measurement of Dislodgement Forces](#) section) were conducted first, followed by trials for the assessing the biomechanics ([Biomechanics of the Implant Region](#) section). Cadavers were kept at room temperature for the duration of each experiment. The biomechanical assessment trials started approximately 15 h post-mortem, the time at which the intensity of rigor mortis was expected to be minimized.<sup>15</sup> The electrode dislodgment trials did not require the full range of motion and therefore were not sensitive to rigor mortis.

### *Biomechanics of the Implant Region*

During movements within the physiological range of motion, the spine and spinal cord move relative to each other.<sup>11</sup> The spinal cord also experiences length changes (elongation or compression) depending on the type of movement. These details are important for the design of a successful strain relief mechanism.

The lumbar enlargement in pigs, the region of interest for the ISMS implant, is located under the L4–L5 vertebrae<sup>10,34</sup> (vs. T11–T12 in humans<sup>27</sup>). This region is similar to the T11–T12 region in humans in two critical aspects: (1) the range of flexion and extension motion—this is 25° in pigs (L3–L6)<sup>38</sup> and 21° to 32° in humans (T10–L1)<sup>24,36</sup>; and (2) the dimensions of the spinal canal—the average width is 20 mm in pigs and 21 mm in humans, and the average depth is 12.5 mm in pigs and 17.5 mm in humans.<sup>30</sup> Furthermore, our gross morphological comparisons of the lumbar enlargement of the spinal cord itself in humans and pigs, suggest that they are similar in size.

A laminectomy was performed between vertebral levels L1–L6 to expose the spinal cord, and the dura mater was opened. Reflective markers were then

attached, using a drop of cyanoacrylate, to the inner walls of the facet joints of each vertebra and to the surface of the spinal cord in the middle of every other facet joint (Fig. 2a). In order to quantify the flexion and extension angles of the spinal column, reflective markers were secured on the sacrum and on the spinous processes of vertebrae T4 and T15 (Fig. 2b). Markers were also placed on the hip, knee, shoulder and elbow joints.

A 3D motion capture system (Vicon Motion Systems Ltd., Oxford, UK) was used to quantify the movements of the spinal cord relative to the spinal column. Six to eight cameras were used to cover a volume of about 1.5 m × 0.8 m × 0.8 m (width × height × depth) (Fig. 2c). Before each experiment, the motion capture system was calibrated for both static and dynamic motions and the measurement error was <0.1 mm. In all of the reported trials, the animal was positioned on its right side on the surgical table. The thoracolumbar spine was moved between neutral, hyperflexion and hyperextension states by bilateral movements of the limbs as shown in Fig. 3. For each trial, the 3D coordinates of the reflective markers were recorded continuously at a rate of 120 frames/s. Therefore, by tracking the kinematics of the animal's spine between hyperflexion and hyperextension, a series of biomechanical data became available for all thoracolumbar angles in this range. The spine neutral position was defined by thoracolumbar angle of 140° consistently across animals (Figs. 3a, 2b). The acquired data were then filtered with a 2nd order low-pass Butterworth filter (cut-off frequency of 12 Hz) before analysis. Data analysis was performed using a custom written Matlab (version R2015a, MathWorks co., Natick, USA) program.

All measurements were associated with the dorsal side of the spinal canal and spinal cord, which are most directly relevant for the lead-wires of the ISMS implants. Also, in all calculations involving the facet joint markers, the coordinates of the markers on the right and left sides of the canal were averaged to find a representative location in the middle (mediolateral direction) of the canal. This is also relevant to the ISMS implants, where the stimulator and bundle of emerging lead wires are attached to the middle of the spinous process, rostral to the implant region (Fig. 1).

### *Measurement of Dislodgement Forces*

Displacements and length changes of the implant region of the spinal cord, collectively referred to as “range of spinal cord movement,” expose the lead wires, and thereby the electrodes, to forces that could cause their dislodgment. Successful lead wire design

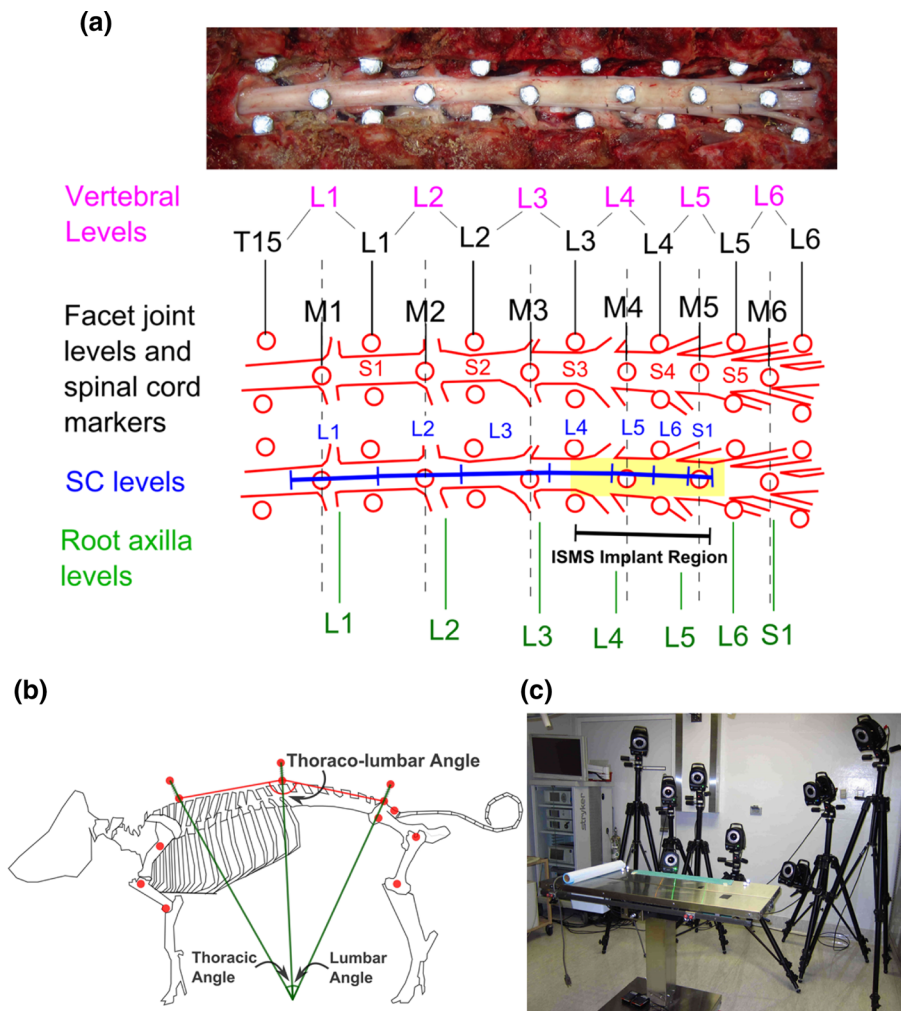


**FIGURE 2.** Reflective markers on the spinal cord and spinal canal. (a) Positions of reflective markers for measurements of the mechanics of the spinal column and spinal cord during physiological movements. The markers on the spinal canal were at the level of the facet joints. The spinal cord markers, placed on the dorsal surface of the spinal cord, were positioned in between the spinal canal markers (rostr-caudally). Spinal cord levels (annotated in blue) were identified by their relationship to the position of the root axilla levels. (b) Positions of the reflective markers on the pig cadaver and definition of the measured angles. (c) Motion capture camera setup with respect to the surgical table. Six to eight cameras were used to cover a volume of about  $1.5 \text{ m} \times 0.8 \text{ m} \times 0.8 \text{ m}$  (width  $\times$  height  $\times$  depth). In all of the reported trials, the animal was positioned on its right side on the surgical table with the reflective markers on its spine and spinal cord facing the cameras.

requires knowledge about the force levels that could dislodge the electrodes from their initial position.

In-Fiber Bragg Grating (FBG) strain sensors<sup>7,8</sup> were placed in line with stiff lead wires connected to ISMS electrodes (Fig. 4a). These sensors are light and relatively small (optical fiber diameter =  $125 \mu\text{m}$ ); therefore, they could readily be incorporated as part of the lead wires in these experiments. Because FBG sensors are also sensitive to temperature changes,<sup>8</sup> a second FBG sensor was placed in close proximity to the force sensor as a reference at all times. Temperature related artefacts were removed from the force measurement recordings by removing the temperature induced signal changes (from the second FBG) from the signal changes of the first (force sensing) FBG. Prior to the

experiments, the FBG sensors were calibrated by measuring the weight of suspended masses ranging from 0.1 to 200 g and were deemed reliable in the range of interest with a coefficient of determination ( $r^2$ ) of 0.9999. Acquired force data were analyzed to determine dislodgment forces using a custom written Matlab program. Statistical analyses were performed using IBM SPSS Statistics software (version 22, IBM Co., Armonk, USA).

#### Bench Testing

Dislodgment forces were first measured in a bench-top setup that simulated the horizontal movement of the lead wire on top of the spinal cord during



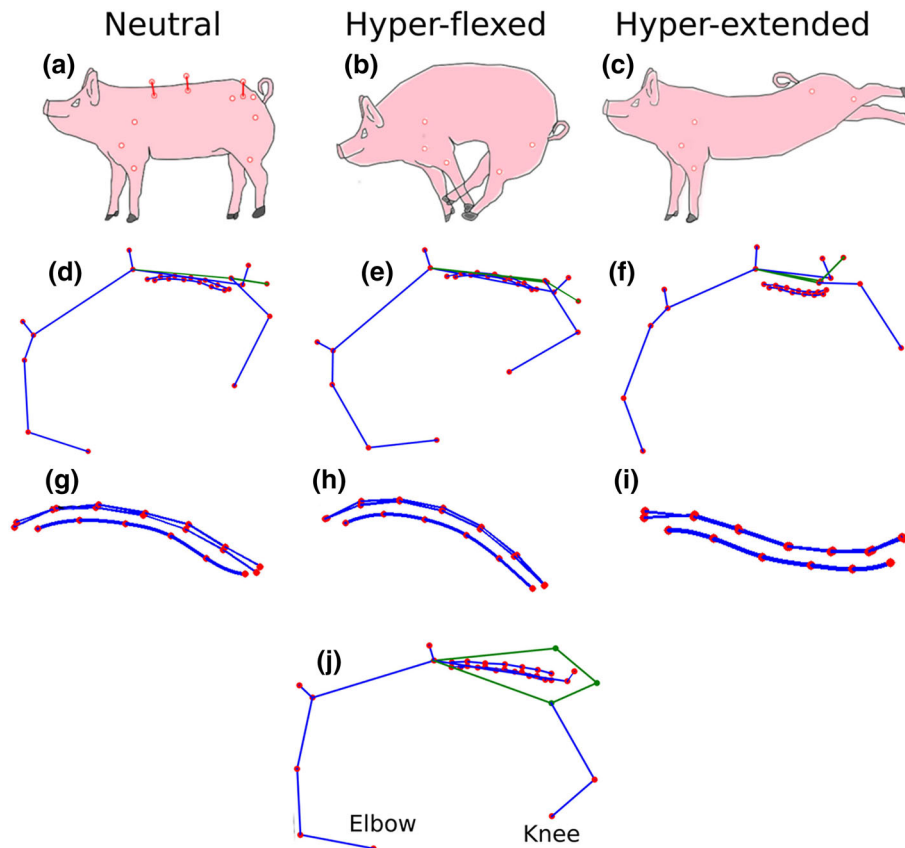


**FIGURE 3.** Changes in marker position during movements within the physiological range of motion. (a) Spine neutral position. (b) Spine hyperflexed position reached by moving both forelimbs caudally and both hind limbs rostrally. (c) Spine hyperextended position reached by moving both hind limbs caudally and dorsally. Spinal canal reflective markers on the facet joints and spinal cord markers in the sagittal plane with the spine in the neutral (d), hyperflexed (e) and hyperextended (f) state. Close up of the spinal cord markers in the sagittal plane with the spine in the neutral state (g), hyperflexed (h) and hyperextended (i) state. (j) 3D view of the reflective markers in the neutral state. The pigs were placed on their right side on a flat surgical table for all trials.

movements (Fig. 4a). Platinum/iridium (Pt/Ir) micro-wires (80% Pt), 50  $\mu\text{m}$  in diameter were bent to 90° close to the tip, leaving a 4.7 mm length between the bend and the tip. The electrode was implanted in surrogate spinal cord materials (tofu<sup>33</sup> and gelatin hydrogel<sup>6</sup>) and its lead portion, along with the FBG sensors laid flush with the cord surface. In order to measure dislodgment forces, a perturbing force was gradually applied in line with the lead wire and the FBG sensor by applying controlled translational movements (Fig. 4a). The forces were recorded continuously at a sampling frequency of 2.5 kHz for the duration of the trial. The effect of electrode insertion angle on the measured dislodgment forces was also investigated in gelatin hydrogel surrogate spinal cords<sup>6</sup> since they were transparent and allowed confirmation of the insertion angles (Fig. 4b).

#### *In-situ Experiments*

Dislodgment forces were also measured *in situ*. A laminectomy was performed at the L3–L6 vertebrae

and the dura mater was opened. In each trial, the ISMS electrode (same as that used in the bench trials, bent to 90°) was implanted into the spinal cord with the lead wire-FBG sensor lying on the dorsal surface of the cord. The sensor's optical fiber was then fixed to the L2 spinous process on its path towards the data recording unit. The implantation protocol was consistent with published ISMS implantation protocols<sup>1,3,20</sup> with the exception of not using mechanically stabilizing components (i.e., cyanoacrylate) at the entry point of the electrode into the spinal cord. The pigs were then moved from the neutral to the hyperflexed and hyperextended positions (Fig. 3b) while recording forces continuously in real time at a sampling frequency of 625 Hz.

#### *Coil Fabrication and Testing*

Based on the information obtained from the pilot experiments in three pig cadavers (the spine-spinal cord mechanics and the dislodgment forces), coils of

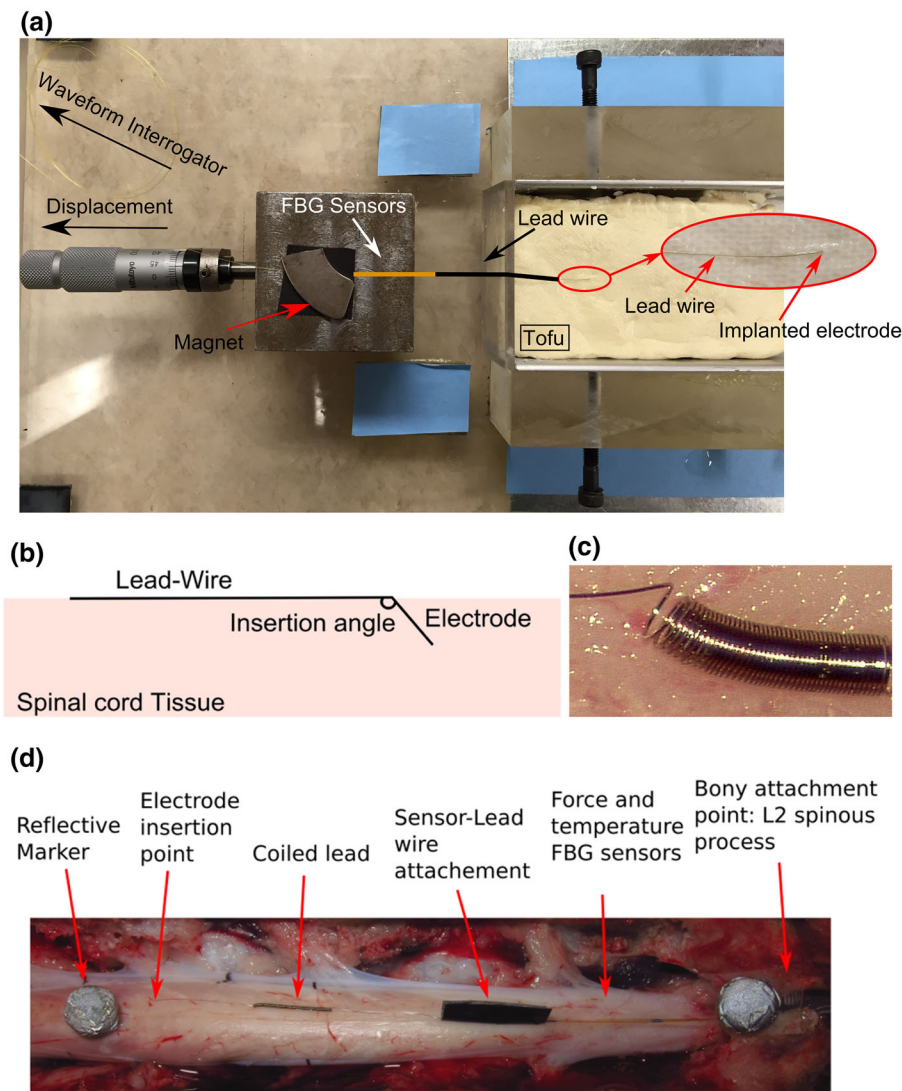


**FIGURE 4.** Bench and *in situ* setups for measurement of electrode dislodgement forces. (a) Bench testing setup shown for a dislodgement trial in Tofu—the thickness of the FBG sensor and the lead wire have been increased to improve their visibility. (b) Electrode insertion angle. (c) A close up image of coil type #3 lying on the dorsal surface of the spinal cord. (d) Experimental setup for testing in fresh pig cadavers. One reflective marker is placed on the lead-sensor fixation point on the bone (L2 spinous process) and another close to the insertion point of the electrode. In this example, a coil is attached in-series to an FBG sensor to measure force and another FBG sensor is also used in parallel for temperature compensation.

varying dimensions and effective mechanical stiffness were designed to provide appropriate strain relief in the lead wire (Table 1). The role of the coils was to eliminate the transmission of forces along the lead wires to the electrodes during physiological movements of the spine. These coils were designed for ISMS implants that were surgically placed with the pig spine in the neutral position (Fig. 3). In this case, coils needed to accommodate approximately 5 mm of range of spinal cord movement without experiencing forces close to the dislodgment threshold. To increase the design safety margin and minimize the forces experienced by the implanted electrodes, the displacement requirement for the coil was doubled to 1 cm. For the

scope of this study, coils were made from two of the most common microwires used in the fabrication of the ISMS arrays: 30 and 50  $\mu\text{m}$  Pt/Ir (80%/20%). The pitch was kept constant and the coil outer diameter was limited to a maximum of 800  $\mu\text{m}$ . These coils were manually constructed from microwires using a lathe for coiling, and hypodermic needles of varying outer diameters as coiling shafts.

Each coil was characterized (force vs. strain profile) using a linear micro-actuator (M-227.50—Physik Instrumente, GMBH & Co., Karlsruhe, Germany) and an FBG sensor. The coil was attached to a static bench clamp on one side and to the FBG sensor and micro-actuator on the other. The micro-actuator strained the

**TABLE 1. Specifications of the fabricated coil types and results of bench characterization and *in situ* testing in fresh pig cadavers.**

Coil type	Wire diameter ( $\mu\text{m}$ )	Coil diameter ( $\mu\text{m}$ )	Coil length (cm)	Mean force–displacement slope obtained from bench-tests (mN/cm) $\pm$ SD	Electrode status after the <i>in situ</i> tests
1	50	800	1	$4.41 \pm 0.6$	In-place
2	25	800	1	$1.0 \pm 0.9$	In-place
3	50	500	1	$7.7 \pm 3.3$	In-place
4	25	500	1	$1.1 \pm 0.49$	In-place
5	25	200	1	$1.2 \pm 0.9$	In-place
6	50	200	1	$67.3 \pm 8.9$	Dislodged in 30% of trials

coil in 20% steps up to 100% (1 cm), and force was statically recorded at each step. Characterized coils were then incorporated in the ISMS lead wires (Fig. 4c) and tested *in situ* to evaluate their dislodgment outcomes. The testing protocol was the same as in “[Measurement of Dislodgement Forces](#)” section

## RESULTS

### *Biomechanics of the Implant Region*

In a total of 26 hyperflexion and 20 hyperextension trials in three fresh pig cadavers (Fig. 3), the thoracolumbar spine was flexed from its neutral position by  $19.25^\circ \pm 0.57^\circ$  (mean  $\pm$  standard error) and extended from its neutral position by  $23.45^\circ \pm 1.2^\circ$ .

Figures 5a and 5b show the segmental length changes of the spinal canal in hyperflexion and hyperextension movements. The length of each segment was calculated as the distance between the locations of the segment markers. The overall change in length of the spinal canal (vertebral levels L1–L6, facet joint marker levels T15–L6) for moving the thoracolumbar spine from hyperextension to hyperflexion was  $2.4 \pm 0.16$  cm (mean  $\pm$  standard error), which was  $14.18 \pm 0.88\%$  longer than its length at the hyperextended position.

The segmental changes in the length of the spinal cord itself were also measured as shown in Figs. 5c and 5d. The length of the spinal cord segments was calculated by fitting a curve to the markers to represent the curvature of the dorsal surface of the spinal cord, and measuring the corresponding arc length for each segment (Fig. 3). The overall change in length of the spinal cord segments as the thoracolumbar spine moved from hyperextension to hyperflexion was  $1.58 \pm 0.18$  cm (mean  $\pm$  standard error), which was  $10.73 \pm 1.14\%$  longer than its length in the hyperextended position. The resulting relative displacement of the spinal cord and spinal canal was also measured as shown in Figs. 5e and 5f. Figure 5f shows the change in the distance between the spinal cord marker and its

closest rostral facet joint marker, for each segment. Figure 5e shows the two-dimensional change in the distance between these markers, calculated by projecting the coordinates of the facet joint markers onto the fit curve to the surface of the spinal cord and measuring their distance from the spinal cord markers.

The ISMS implant region in pigs is located approximately between facet markers L3–L5 and spinal cord markers M3–M5 (Fig. 2a). In a lumbar ISMS implant in this model, the bundle of lead wires would be fixed to the L2 spinous process, and the electrodes would be implanted in different locations within the M3–M5 region. The worst-case scenario (largest range of coil movement) in terms of stability would be for an electrode implanted most caudally, near the M5 marker. The overall movement range that the lead wire should be able to accommodate without dislodgment of an electrode in this location can be calculated by summing the maximal change in spinal cord length in this region (M3–M5) and the relative displacement of the lamina L2 (bony fixation point) and its adjacent spinal cord marker (M3). These values were  $5.64 \pm 0.59$  and  $5.66 \pm 0.57$  mm, respectively.

In this study, coils were designed and tested for the case when the ISMS implant is surgically placed with the pig’s spine in the neutral position (as opposed to hyperextended position). In this case, the maximal length change of the implant region and the relative displacement of the lamina L2 and the spinal cord marker M3 are  $1.46 \pm 0.39$  and  $2.13 \pm 0.38$  mm, respectively.

### *Measurement of Dislodgement Forces*

Examples of force recordings while translational movements were applied to electrodes implanted in gelatin surrogate spinal cords are shown in Fig. 6a. The average dislodgment force of electrodes implanted in the gelatin surrogate cord was  $30.9 \pm 13$  mN (mean  $\pm$  standard deviation), obtained across 30 trials in three cord samples (Fig. 6b). In comparison, the average force for dislodging electrodes from the tofu

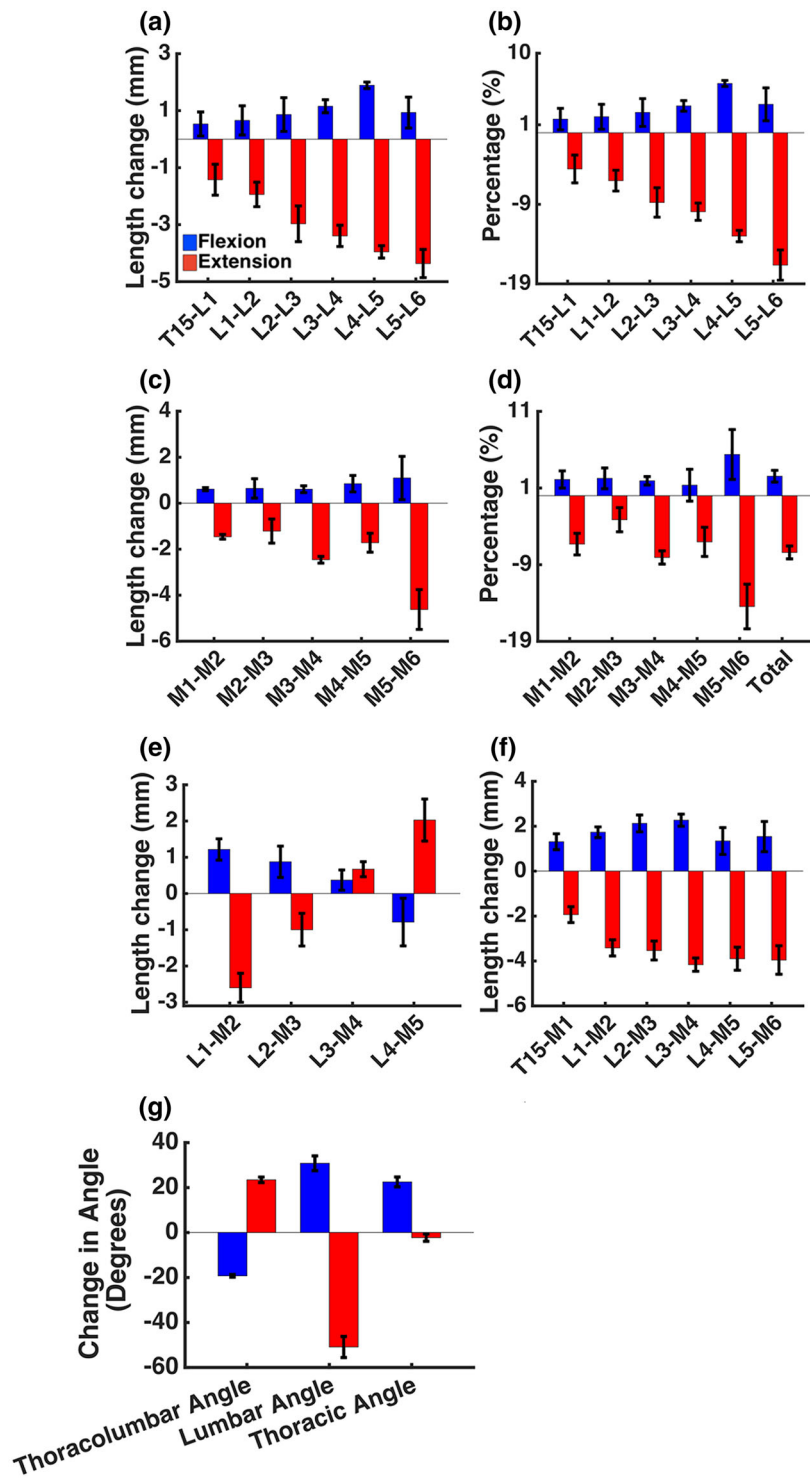
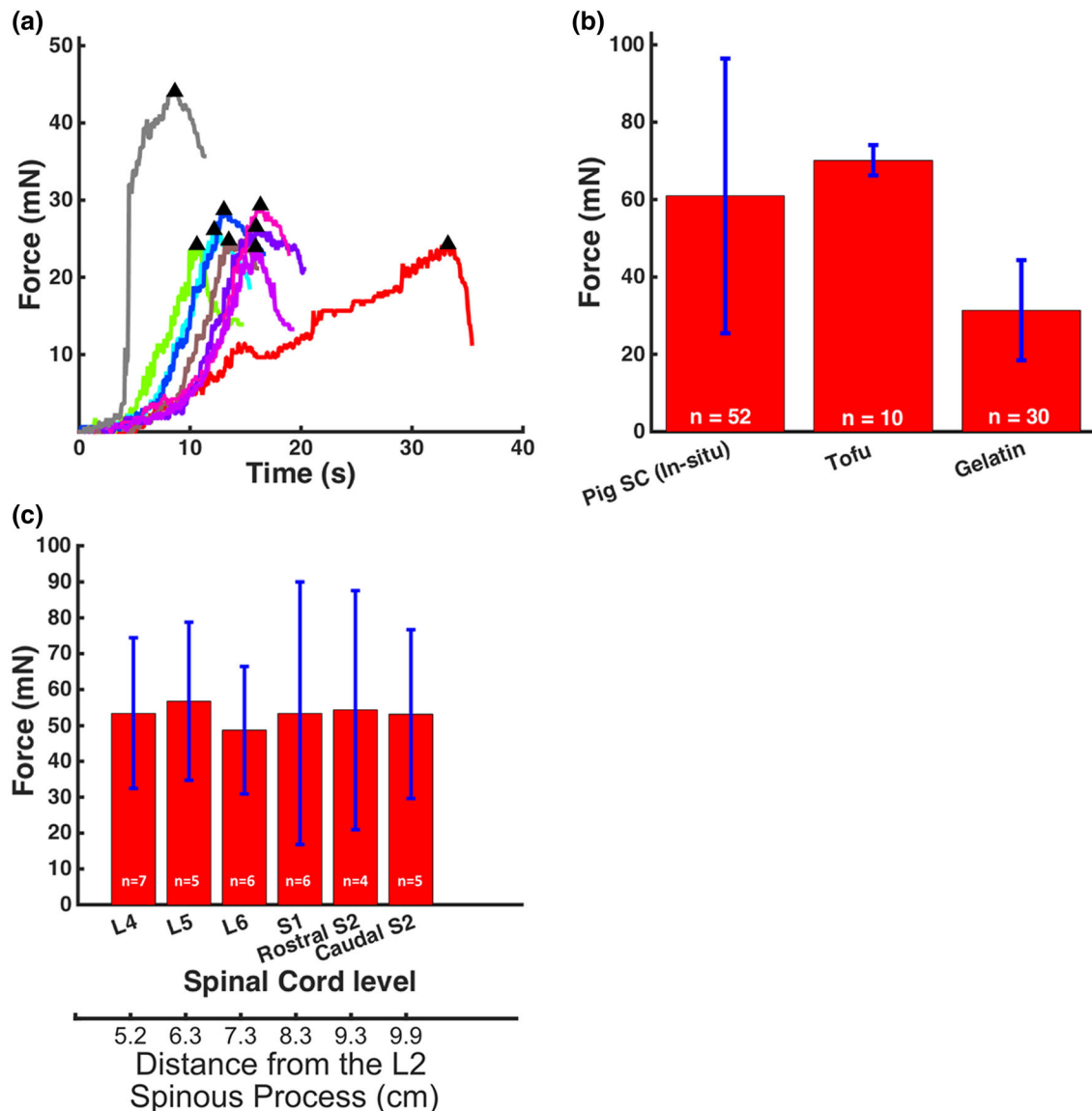


FIGURE 5. Biomechanics of the lumbar spinal cord and canal in fresh pig cadavers. All of the parameters for spine flexion and extension movements were measured with respect to the pig’s neutral position, and all measurements were made on the dorsal side of the spinal cord and canal. (a) Absolute change in the length of spinal canal segments. (b) Change in the length of spinal canal segments relative to their initial length. (c) Absolute measurements of change in length of the spinal cord segments (as defined in Fig. 4). (d) Segmental strain of the spinal cord. (e) Projected displacement of the spinal cord and the spinal canal. This is measured as the change in the distance between the spinal cord marker and the projected position of the spinal canal marker onto the spinal cord surface. This parameter is independent of canal depth and is compatible with the classical measurement methods in literature.<sup>18</sup> (f) Displacement of the spinal cord and the spinal canal. This is measured by the change in the 3D distance between the spinal cord and the spinal canal markers. This parameter is more applicable to the definition of the design constraints required for an ISMS implant. (g) Measured changes in angles from neutral to hyperflexion and hyperextension. The thoracolumbar angle for neutral position was 140°.





**FIGURE 6.** Summary of electrode dislodgment forces obtained without coils in the lead wires. (a) Raw force traces measured in gelatin surrogate spinal cords. As ‘time’ progressed in these trials, more translational movement was applied manually to the lead wires (Fig. 4a) causing an increase in force transmitted to the electrode, until the electrode dislodged (triangle symbols) from its implanted location. Separations of traces in *x*-axis represent variations in the speed of the manual displacements. (b) Average dislodgment forces in tofu and gelatin surrogate cord materials measured in bench-top trials and *in situ* in three fresh pig cadavers obtained while moving the pigs from neutral to hyperflexion (mean  $\pm$  standard error). (c) Effect of implantation location on dislodgment forces. In this experiment, electrodes were implanted in a 4.7 cm-long region of the spinal cord (L4 to S2 spinal cord levels). Implantation location did not have a significant impact on the force threshold for electrode dislodgment. ‘n’ is the number of trials in each experiment.

surrogate spinal cord across 10 trials in two samples was  $70.0 \pm 3.6$  mN (mean  $\pm$  standard deviation).

The electrode insertion angle had a significant effect on the dislodgment force of electrodes implanted in gelatin surrogate cords. In these experiments, the electrodes were implanted at  $45^\circ$  (8 trials),  $90^\circ$  (28 trials) and  $135^\circ$  (17 trials) angles, and the mean dislodgment forces were  $103.5 \pm 19.7$ ,  $33.3 \pm 10.9$  and  $17.3 \pm 6.1$  mN (mean  $\pm$  standard deviation), respec-

tively. The dislodgment forces were significantly different for insertion angles  $45^\circ$ ,  $90^\circ$  and  $135^\circ$  ( $p < 0.001$  for all pairs; Brown-Forsythe corrected statistics and Tamhane’s T2 post hoc analysis).

The average dislodgment force across 52 trials of electrodes implanted with an insertion angle of  $90^\circ$  in the lumbosacral region of the spinal cord in three fresh pig cadavers was  $60.9 \pm 35.5$  mN (mean  $\pm$  standard deviation) (Fig. 6b). Electrode location along the

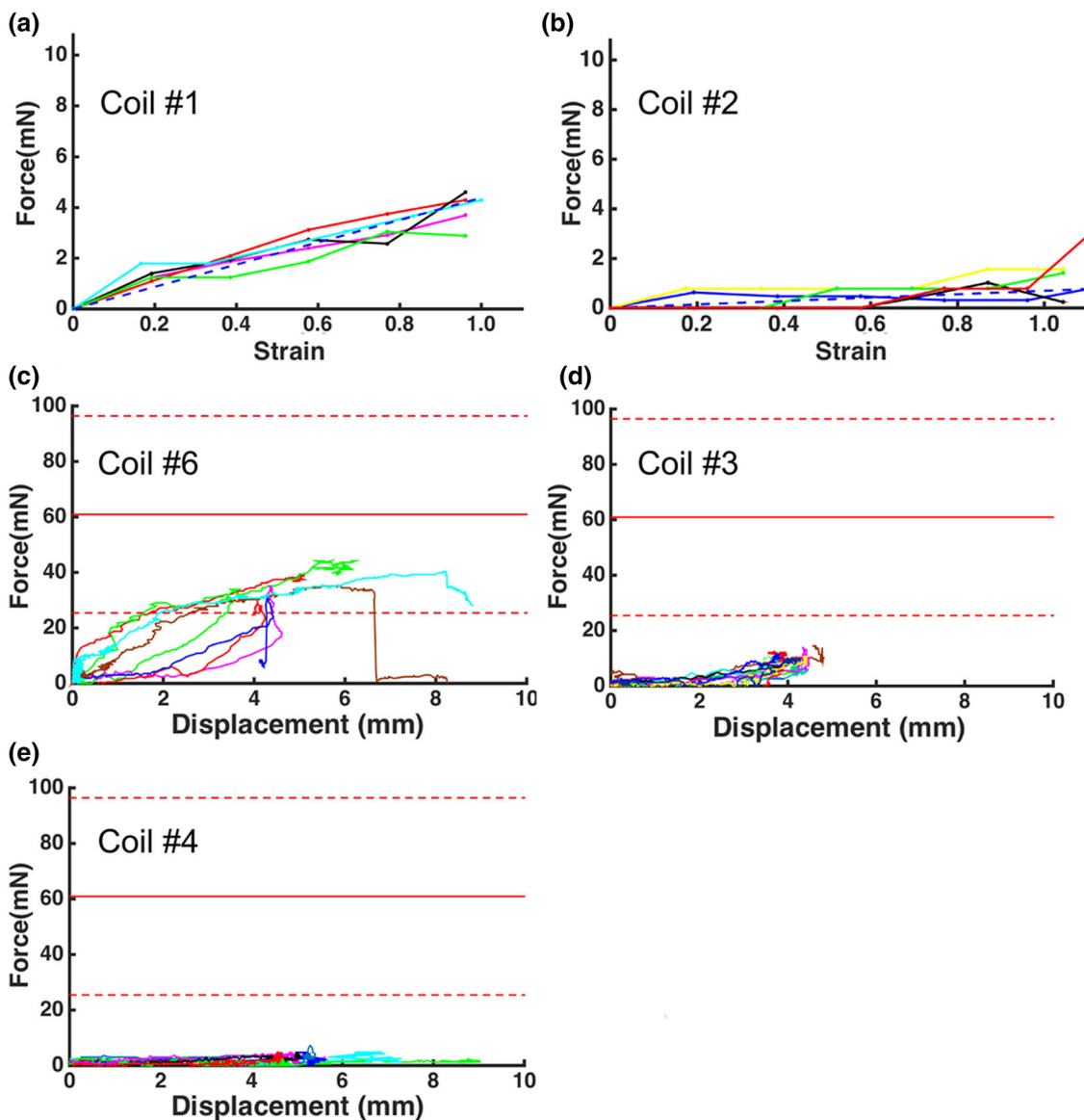


**FIGURE 7.** Force vs. strain and displacement profiles of different coils obtained from bench and *in situ* tests. (a), (b), repeated bench trials (as described in [Coil Fabrication and Testing](#) section) of type #1 ( $n = 5$ ) and type #2 ( $n = 6$ ) coils (Table 1), respectively. Dashed blue lines represent the average of the linear fit-curves of each trial for that coil. (c) Example of results obtained from coils type #6 tested *in situ* ( $n = 8$ ). Electrodes were dislodged in trials shown in brown, cyan and blue. (d) Example of results obtained from coils type #3 tested *in situ* ( $n = 10$ ). (e) Example of results obtained from coils type #4 tested *in situ* ( $n = 13$ ). During *in situ* tests, the pig spine was moved from neutral to hyperflexion. The horizontal red lines in (c), (d) and (e) represent the average minimal dislodgment forces measured without coils *in situ* in pig cadavers, and the horizontal dashed lines represent  $\pm 1$  standard deviation from the average.

region of interest in the spinal cord did not have a significant effect (one-way ANOVA,  $p = 0.998$ ) on the dislodgment forces (Fig. 6c).

#### Coil Fabrication and Testing

Six coil types were fabricated and characterized prior to testing *in situ* in three fresh pig cadavers. Force-strain profiles of two typical coils of types #1 and #2 (Table 1) are shown in Figs. 7a and 7b. Based

on the force-strain profiles obtained during bench testing for each coil type and assuming that the implant region, and therefore the coils incorporated in the lead wires, have a movement range of 1 cm, the maximal force transferred to the implanted electrodes was calculated. These values were then compared to the dislodgement thresholds (mean  $\pm$  standard deviation) measured *in situ*.

Based on bench test results, coil types #1 through #5 (Table 1) were not expected to transmit forces that

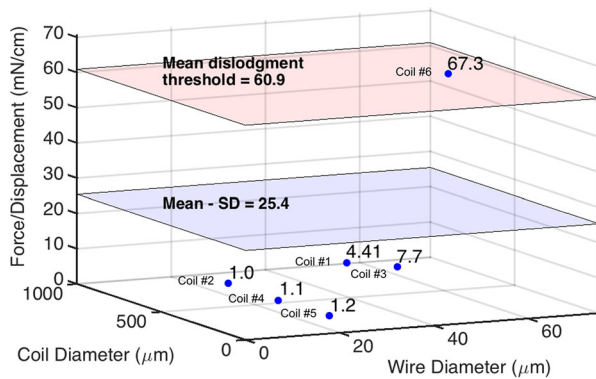


**FIGURE 8.** Summary of coil design specifications and average *in situ* test dislodgment outcomes. The force/displacement profiles shown in this figure are obtained from the bench tests. The red plane represents the mean electrode dislodgment forces measured without coils in pig cadavers and the blue plane shows mean  $-1 \times$  standard deviation. All electrodes attached to coil types #1 through #5 (Table 1) remained in place, while 30% of the electrodes attached to coil type #6 were dislodged when the spine moved from neutral to hyperflexion.

would dislodge the electrodes during *in situ* tests in pig cadavers. Coil type #6, however, was predicted to cause electrode dislodgement as its force-strain profile showed forces higher than the minimal dislodgment forces within the tested strain window.

A total of 78 coils (coil #1:  $n = 11$ , coil #2:  $n = 12$ , coil #3:  $n = 21$ , coil #4:  $n = 10$ , coil #5:  $n = 11$ , coil #6:  $n = 13$ ) were tested *in situ* and the force transmitted to the electrodes were measured. The outcomes were consistent with the predictions made based on bench test results: all tested coils from types #1 through #5 allowed the ISMS electrodes to remain in place without displacement or dislodgement. However, 30% of the coils from type #6 caused their respective ISMS electrodes to dislodge during hyperflexion movements of the spine. Examples of the force-displacement curves recorded during *in situ* dislodgment tests are shown in Figs. 7c–7e. A summary of the average maximal force experienced by the ISMS electrodes for all coil types is shown in Fig. 8.

## DISCUSSION

### Overview

Successful performance of neural implants in the central nervous system may be affected by the tissue's foreign body response (FBR) as a result of factors such as material, shape and relative motion of the implanted electrodes.<sup>35</sup> Many studies have focused on minimizing the FBR by addressing one or more of its contributing factors. This has led to the emergence of various electrode/electrode array designs (e.g., Michigan

microelectrode system,<sup>14</sup> Utah electrode array,<sup>28</sup> Moxon electrode array,<sup>19</sup> Giszter braided electrode<sup>13</sup>) as well as electrode coatings.<sup>39</sup> Among the factors contributing to FBR, “tethering” of the implanted electrodes is shown to be the most important.<sup>9</sup> The focus of this study was on designing a strain relief mechanism that would mechanically decouple the implanted floating electrodes from the fixed stimulator. For the systematic design of such strain relief mechanism, detailed knowledge of the biomechanics of the spinal column and spinal cord during physiological movements was needed. Moreover, knowledge of the forces that could displace electrodes and dislodge them from their site of implantation was also needed. This information was obtained in the present study, and coils that accommodated for the movement range experienced by the spinal cord during physiological movements were successfully designed and tested.

### Similarity Between the Biomechanics of the Spine in Humans and Pigs

A comparison between the results presented here and a meticulous study conducted by Louis<sup>17</sup> in fresh human cadavers demonstrates similarities in all of the measured relevant biomechanical variables. For instance, Louis<sup>17</sup> reported the overall change in length of the lumbar spinal canal to be 2.8 cm in humans (measured from spine neutral to hyperflexion positions) while this study found it to be  $2.4 \pm 0.16$  cm in the domestic pig model. With regards to the ISMS implant region (vertebral levels L4–L5 in pigs and T11–T12 in humans), the overall length change of the spinal cord in pigs was  $5.64 \pm 0.59$  mm. In Louis's study,<sup>17</sup> the overall elongation of the spinal cord under vertebral levels T11–T12 in humans was approximately 7.5 mm (hyperflexion with respect to hyperextension positions). In both studies, similar trends were observed in the direction of the relative displacement of the spinal cord and spinal canal. Results in Fig. 5e suggest that during spine flexion, the direction of spinal cord displacement with respect to the spinal canal changes at the L3–L4 intervertebral disc. Louis's results suggest that this change occurs at intervertebral disc L4–L5 in humans.<sup>17</sup>

Larger length changes are observed in extension movements than flexion in pigs than in humans (Fig. 5). This is partly because of the difference in the neutral positions and inherent differences in the lordosis angles in the human and pig lumbar spines:  $29.2 \pm 7.6^\circ$  in humans and  $7.9 \pm 5.7^\circ$  in pigs.<sup>5</sup> Nonetheless, taken collectively, the results obtained in this study confirm the assumption that domestic pigs are an appropriate large animal model for humans,

particularly for the assessment of the mechanical stability of lumbar ISMS implants.

In the present study, we also successfully measured the minimal force levels (thresholds) for dislodging 4.7 mm long ISMS electrodes implanted in pig spinal cords. Results shown in Fig. 6c suggest that these values are not location dependent within the lumbar spinal cord. However, the insertion angle of the electrodes had a significant effect on thresholds for electrode dislodgement, suggesting that it is an important design parameter for mechanical stability of ISMS implants.

Based on bench testing in surrogate spinal cord materials, gelatin hydrogel cords<sup>6</sup> had the lowest thresholds for electrode dislodgement. This suggests that these cords may be an excellent test tool for future bench testing since implanted systems that pass the dislodgment requirements in these cords are expected to perform within the design parameters *in situ*.

Dislodgment forces measured *in situ* demonstrated a larger variability compared with measurements obtained from surrogate cords in the bench tests (Fig. 6b). This may be because the topography of the dorsal surface of the spinal cord and its overlying vessels is less uniform than that of the surrogate cord materials; thus resulting in larger variabilities in friction and *in situ* dislodgment forces. Coil types that passed the *in situ* dislodgment tests provide examples of specifications of suitable coils for a mechanically stable ISMS implant.

#### *Design Implications for Human Implants*

Based on the results obtained in this study, domestic pigs are an appropriate animal model for testing the mechanical stability of human lumbar ISMS implants. An important consideration for the design of ISMS implants is the difference in the spine neutral positions of humans and pigs, which has important implications for the ranges of elongation and compression for coil testing. For instance, coiled lead wires that would be surgically implanted in humans in a prone position can experience larger elongations than those implanted in the pig's neutral position. Since spine surgeries are commonly performed with patients in the prone position, for best compatibility, coiled lead wires should be designed and surgically implanted in pigs while in an extended spine position.

The range of coil movement as a design constraint should be selected to be larger than 12.11 mm for an ISMS implant in pigs. Past studies in humans did not directly characterize all the relevant variables for the ISMS implant region (e.g., 3D displacement of the spinal cord with respect to the neighbouring lamina as shown in Fig. 5f). However, similarities between the implant regions of pigs and humans suggest the pos-

sibility of using the same critical value with a correction factor to increase the design safety margin, until direct measurements in humans become available. Another reason for the use of an appropriate correction factor is the limitations associated with the scope of this study. For instance, we have only investigated extreme conditions for the thoracolumbar spine flexion/extension movements and have not considered more complex combinatory movements (e.g., addition of cervical spine movements or axial rotation and lateral bending of the spine) which could potentially produce larger displacements and length changes in the implant region.<sup>11</sup>

In the design of an appropriate coil, the critical movement range of the implant region should account for both elongation and compression of the spinal cord relative to the neutral (prone) position. For instance, the coils that were designed in this study for placement with the pig in neutral position should be able to accommodate at least 8.3 mm of compression and 4.1 mm of elongation (overall movement range of 12.1 mm, Figs. 5c, 5f). Although compression tests were not conducted in this study, future designs should include these tests as well.

The critical force limit as a coil design constraint should be lower than the minimal dislodgment forces measured in pig spinal cords (mean  $- 1 \times$  standard deviation = 25.4 mN) to ensure implant stability. Because the implanted ISMS electrodes go through the pia mater, the coils should be softer than the pia mater to minimize the electrode's micromotion in the spinal cord. The Young's modulus of the spinal cord pia mater is 2.3 MPa and the spinal cord itself has a Young's modulus of 5 kPa.<sup>25</sup>

The equivalent Young's modulus of springs/coils can be calculated from<sup>32</sup>:

$$\frac{\text{Force}}{\text{Coil cross sectional area}} = E \frac{\Delta L}{L}$$

where  $E$  is the Young's modulus and  $L$  is the coil length. For instance, the equivalent Young's modulus of coil type #2 at 100% strain, is  $\sim 2$  kPa which is 1150 times lower than the pia mater's modulus and 2.5 times lower than the spinal cord's modulus. Based on the results obtained in this study, coiled lead-wires can be designed to ensure mechanical stability and resemble an untethered condition of the implanted ISMS electrodes as closely as possible.

To the best of our knowledge, the dislodgment forces measured in this study are the first for any spinal cord implant in any species. Therefore, although we do not believe that these forces would be different in humans, correction factors should be used to account for potential variations between species, until measured directly.



Consistency of the *in situ* coil test outcomes with the predictions made based on the design constraints demonstrates the reliability of the utilized methods (biomechanics and dislodgement force measurements) for the systematic design of a mechanically stable ISMS implant. These techniques may also be applied for the design of any mechanically stable neural implant.

Length changes of the spinal cord resulting from extreme movements also result in elastic deformation of the spinal cord cross-section. In order to minimize the potential effect of such disturbances to the implanted electrodes, an ideal ISMS implant should also consist of electrodes with mechanical properties matching those of the spinal cord, in addition to the lead-wire design considerations presented in the present study.

### CONCLUSIONS

In this study, we investigated the design constraints for a mechanically stable lumbar ISMS implant driven mainly by the design of the lead wires. In a domestic pig model, we measured the effect of hyperflexion and hyperextension movements of the thoracolumbar spine on the length changes and relative displacements of the ISMS implant region. The results suggested that domestic pigs are a suitable model for humans for testing lumbar ISMS implants. Electrode dislodgement forces were then measured in pig cadavers. These constraints were used to design a strain relief mechanism in the lead wire that can dissociate the implanted electrode from the rest of the implant.

As a proof of concept, six types of coiled lead wires were fabricated, characterized and tested in pig cadavers. These coils substantially reduced the forces transmitted to the electrode, preventing its dislodgement from the tissue. Future studies will focus on testing the long-term mechanical stability of chronically implanted ISMS systems in pigs.

### ACKNOWLEDGMENTS

The authors thank Mr. Robert Butz for assistance with early measurement of electrode dislodgement forces, and Mr. Theodore Ng and Dr. Anastasia Elias for assistance in preparing surrogate spinal cords. Funding for this work was provided by the Canadian Institutes of Health Research, the Natural Sciences and Engineering Research Council of Canada and Alberta Innovates – Health Solutions (AIHS). AT was supported by a Vanier Canada Graduate Scholarship and an AIHS Graduate Studentship. VKM was an Alberta Heritage Foundation for Medical Research Senior Scholar.

### REFERENCES

- <sup>1</sup>Bamford, J. A., R. M. Lebel, K. Parseyan, and V. K. Mushahwar. The fabrication, implantation and stability of intraspinal microwire arrays in the spinal cord of cat and rat. *Trans. Neural Syst. Rehabil. Eng.* 2016.
- <sup>2</sup>Bamford, J. A., C. T. Putman, and V. K. Mushahwar. Intraspinal microstimulation preferentially recruits fatigue-resistant muscle fibres and generates gradual force in rat. *J. Physiol.* 569:873–884, 2005.
- <sup>3</sup>Bamford, J. A., K. G. Todd, and V. K. Mushahwar. The effects of intraspinal microstimulation on spinal cord tissue in the rat. *Biomaterials* 31:5552–5563, 2010.
- <sup>4</sup>Biran, R., D. C. Martin, and P. A. Tresco. The brain tissue response to implanted silicon microelectrode arrays is increased when the device is tethered to the skull. *J. Biomed. Mater. Res. A* 82:169–178, 2007.
- <sup>5</sup>Busscher, I., J. J. W. Ploegmakers, G. J. Verkerke, and A. G. Veldhuizen. Comparative anatomical dimensions of the complete human and porcine spine. *Eur. Spine J.* 19:1104–1114, 2010.
- <sup>6</sup>Cheng, C., J. Kmech, V. K. Mushahwar, and A. L. Elias. Development of surrogate spinal cords for the evaluation of electrode arrays used in intraspinal implants. *IEEE Trans. Biomed. Eng.* 60:1667–1676, 2013.
- <sup>7</sup>Dennison, C. R., P. M. Wild, D. R. Wilson, and P. A. Cripton. A minimally invasive in-fiber Bragg grating sensor for intervertebral disc pressure measurements. *Meas. Sci. Technol.* 19:085201, 2008.
- <sup>8</sup>Dennison, C. R., P. M. Wild, D. R. Wilson, and M. K. Gilbert. An in-fiber Bragg grating sensor for contact force and stress measurements in articular joints. *Meas. Sci. Technol.* 21:115803, 2010.
- <sup>9</sup>Ersen, A., S. Elkabes, D. S. Freedman, and M. Sahin. Chronic tissue response to untethered microelectrode implants in the rat brain and spinal cord. *J. Neural Eng.* 12:016019, 2015.
- <sup>10</sup>Hachmann, J. T., J. H. Jeong, P. J. Grahn, G. W. Mallory, L. Q. Evertz, A. J. Bieber, D. A. Lobel, K. E. Bennet, K. H. Lee, and J. L. Lujan. Large animal model for development of functional restoration paradigms using epidural and intraspinal stimulation. *Plos One* 8:e81443, 2013.
- <sup>11</sup>Harrison, D. E., R. Cailliet, D. D. Harrison, S. J. Troyanovich, and S. O. Harrison. A review of biomechanics of the central nervous system—part II: spinal cord strains from postural loads. *J. Manip. Physiol. Ther.* 22:322–332, 1999.
- <sup>12</sup>Holinski, B. J. Restoring walking after spinal cord injury. 2013. <<https://era.library.ualberta.ca/public/view/itcm/uid:0e698e79-b16a-4519-baf7-552a49dda767/>>.
- <sup>13</sup>Kim, T., A. Branner, T. Gulati, and S. F. Giszter. Braided multi-electrode probes: mechanical compliance characteristics and recordings from spinal cords. *J. Neural Eng.* 10:045001, 2013.
- <sup>14</sup>Kipke, D. R., R. J. Vetter, J. C. Williams, and J. F. Hetke. Silicon-substrate intracortical microelectrode arrays for long-term recording of neuronal spike activity in cerebral cortex. *IEEE Trans. Neural Syst. Rehabil. Eng. Publ. IEEE Eng. Med. Biol. Soc.* 11:151–155, 2003.
- <sup>15</sup>Krompecher, T. Experimental evaluation of rigor mortis V. Effect of various temperatures on the evolution of rigor mortis. *Forensic Sci. Int.* 17:19–26, 1981.
- <sup>16</sup>Lau, B., L. Guevremont, and V. K. Mushahwar. Strategies for generating prolonged functional standing using intramuscular stimulation or intraspinal microstimulation.

- IEEE Trans. Neural Syst. Rehabil. Eng. Publ. IEEE Eng. Med. Biol. Soc.* 15:273–285, 2007.
- <sup>17</sup>Louis, R. Vertebro-radicular and vertebromedullar dynamics. *Anat. Clin.* 3:1–11, 1981.
- <sup>18</sup>McConnell, G. C., H. D. Rees, A. I. Levey, C. A. Gutekunst, R. E. Gross, and R. V. Bellamkonda. Implanted neural electrodes cause chronic, local inflammation that is correlated with local neurodegeneration. *J. Neural Eng.* 6:056003, 2009.
- <sup>19</sup>Moxon, K. A., S. C. Leiser, G. A. Gerhardt, K. A. Barbee, and J. K. Chapin. Ceramic-based multisite electrode arrays for chronic single-neuron recording. *IEEE Trans. Biomed. Eng.* 51:647–656, 2004.
- <sup>20</sup>Mushahwar, V. K., D. F. Collins, and A. Prochazka. Spinal cord microstimulation generates functional limb movements in chronically implanted cats. *Exp. Neurol.* 163:422–429, 2000.
- <sup>21</sup>Mushahwar, V. K., and K. W. Horch. Selective activation of muscle groups in the feline hindlimb through electrical microstimulation of the ventral lumbo-sacral spinal cord. *IEEE Trans. Rehabil. Eng.* 8:11–21, 2000.
- <sup>22</sup>Nashold, B. S., H. Friedman, J. F. Glenn, J. H. Grimes, W. F. Barry, and R. Avery. Electromycturition in paraplegia. Implantation of a spinal neuroprosthesis. *Arch. Surg. Chic. Ill 1960* 104:195–202, 1972.
- <sup>23</sup>Nashold, B. S., J. Grimes, H. Friedman, J. Semans, and R. Avery. Electrical stimulation of the conus medullaris in the paraplegic. A 5-year review. *Appl. Neurophysiol.* 40:192–207, 1977.
- <sup>24</sup>Oxland, T. R., R. M. Lin, and M. M. Panjabi. Three-dimensional mechanical properties of the thoracolumbar junction. *J. Orthop. Res. Off. Publ. Orthop. Res. Soc.* 10:573–580, 1992.
- <sup>25</sup>Ozawa, H., T. Matsumoto, T. Ohashi, M. Sato, and S. Kokubun. Mechanical properties and function of the spinal pia mater. *J. Neurosurg. Spine* 1:122–127, 2004.
- <sup>26</sup>Peckham, P. H., and J. S. Knutson. Functional electrical stimulation for neuromuscular applications. *Annu. Rev. Biomed. Eng.* 7:327–360, 2005.
- <sup>27</sup>Purves, D., G. J. Augustine, D. Fitzpatrick, L. C. Katz, A. S. LaMantia, J. O. McNamara, and S. M. Williams. The external anatomy of the spinal cord. In: *Neuroscience*. Sunderland: Sinauer Associates, 2001. <<http://www.ncbi.nlm.nih.gov/books/NBK11160/>>.
- <sup>28</sup>Rousche, P. J., and R. A. Normann. Chronic recording capability of the Utah intracortical electrode array in cat sensory cortex. *J. Neurosci. Methods* 82:1–15, 1998.
- <sup>29</sup>Saigal, R., C. Renzi, and V. K. Mushahwar. Intraspinal microstimulation generates functional movements after spinal-cord injury. *IEEE Trans. Neural Syst. Rehabil. Eng.* 12:430–440, 2004.
- <sup>30</sup>Sheng, S. R., X. Y. Wang, H. Z. Xu, G. Q. Zhu, and Y. F. Zhou. Anatomy of large animal spines and its comparison to the human spine: a systematic review. *Eur. Spine J.* 19:46–56, 2010.
- <sup>31</sup>Smit, T. H. The use of a quadruped as an *in vivo* model for the study of the spine—biomechanical considerations. *Eur. Spine J.* 11:137–144, 2002.
- <sup>32</sup>Smith, J. O. *Physical Audio Signal Processing*. New York: W3K Publishing, 2010.
- <sup>33</sup>Snow, S., S. C. Jacobsen, D. L. Wells, and K. W. Horch. Microfabricated cylindrical multielectrodes for neural stimulation. *IEEE Trans. Biomed. Eng.* 53:320–326, 2006.
- <sup>34</sup>Szentkuti, L., and J. Bruns. Motoneurons of M. semitendinosus in domestic and wild pigs. A horseradish peroxidase and cord-survey study. *Anat. Embryol. (Berl.)* 167:213–228, 1983.
- <sup>35</sup>Ward, M. P., P. Rajdev, C. Ellison, and P. P. Irazoqui. Toward a comparison of microelectrodes for acute and chronic recordings. *Brain Res.* 1282:183–200, 2009.
- <sup>36</sup>White, A. A., and M. Panjabi. *Clinical Biomechanics of the Spine*. Philadelphia: Wolters Kluwer, p. 722, 1990.
- <sup>37</sup>WHO Spinal cord injury. <<http://www.who.int/mediacentre/factsheets/fs384/en/>>.
- <sup>38</sup>Wilke, H. J., J. Geppert, and A. Kienle. Biomechanical in vitro evaluation of the complete porcine spine in comparison with data of the human spine. *Eur. Spine J.* 20:1859–1868, 2011.
- <sup>39</sup>Zhong, Y., and R. V. Bellamkonda. Dexamethasone-coated neural probes elicit attenuated inflammatory response and neuronal loss compared to uncoated neural probes. *Brain Res.* 1148:15–27, 2007.